FDTD simulation of transmittance characteristics of one-dimensional conducting electrodes

Kilbock Lee,[1] Seok Ho Song,[2] and Jinho Ahn[1,*]

[1]*Department of Material Science and Engineering, Hanyang University, 222 Wangsimni-ro, Seongdong-gu, Seoul, 133-791, South Korea*

[2]*Department of Physics, Hanyang University, 222 Wangsimni-ro, Seongdong-gu, Seoul, 133-791, South Korea*

[*]*jhahn@hanyang.ac.kr*

Abstract: We investigated transparent conducting electrodes consisting of periodic one-dimensional Ag or Al grids with widths from 25 nm to 5 μm via the finite-difference time-domain method. To retain high transmittance, two grid configurations with opening ratios of 90% and 95% were simulated. Polarization-dependent characteristics of the transmission spectra revealed that the overall transmittance of micron-scale grid electrodes may be estimated by the sum of light power passing through the uncovered area and the light power penetrating the covered metal layer. However, several dominant physical phenomena significantly affect the transmission spectra of the nanoscale grids: Rayleigh anomaly, transmission decay in TE polarized mode, and localized surface plasmon resonance. We conclude that, for applications of transparent electrodes, the critical feature sizes of conducting 1D grids should not be less than the wavelength scale in order to maintain uniform and predictable transmission spectra and low electrical resistivity.

OCIS codes: (160.2100) Electro-optical materials; (310.6628) Subwavelength structures, nanostructures; (310.6805) Theory and design; (310.7005) Transparent conductive coatings.

References and links

1. D. S. Hecht, L. Hu, and G. Irvin, "Emerging Transparent Electrodes Based on Thin Films of Carbon Nanotubes, Graphene, and Metallic Nanostructures," Adv. Mater. **23**(13), 1482–1513 (2011).
2. P. B. Catrysse and S. Fan, "Nanopatterned metallic films for use as transparent conductive electrodes in optoelectronic devices," Nano Lett. **10**(8), 2944–2949 (2010).
3. J. van de Groep, P. Spinelli, and A. Polman, "Transparent conducting silver nanowire networks," Nano Lett. **12**(6), 3138–3144 (2012).
4. L. Hu, D. S. Hecht, and G. Grüner, "Percolation in Transparent and Conducting Carbon Nanotube Networks," Nano Lett. **4**(12), 2513–2517 (2004).
5. I. Khrapach, F. Withers, T. H. Bointon, D. K. Polyushkin, W. L. Barnes, S. Russo, and M. F. Craciun, "Novel highly conductive and transparent graphene-based conductors," Adv. Mater. **24**(21), 2844–2849 (2012).
6. A. R. Madaria, A. Kumar, and C. Zhou, "Large scale, highly conductive and patterned transparent films of silver nanowires on arbitrary substrates and their application in touch screens," Nanotechnology **22**(24), 245201 (2011).
7. M. G. Kang, T. Xu, H. J. Park, X. Luo, and L. J. Guo, "Efficiency enhancement of organic solar cells using transparent plasmonic Ag nanowire electrodes," Adv. Mater. **22**(39), 4378–4383 (2010).
8. L. Hu, H. Wu, and Y. Cui, "Metal nanogrids, nanowires, and nanofibers for transparent electrodes," MRS Bull. **36**(10), 760–765 (2011).
9. K. Ellmer, "Past achievements and future challenges in the development of optically transparent electrodes," Nat. Photonics **6**(12), 809–817 (2012).
10. A. Seh-Won, L. Ki-Dong, K. Jin-Sung, K. Sang Hoon, P. Joo-Do, L. Sarng-Hoon, and Y. Won, "Fabrication of a 50 nm half-pitch wire grid polarizer using nanoimprint lithography," Nanotechnology **16**(9), 1874–1877 (2005).
11. T. W. Ebbesen, H. J. Lezec, H. F. Ghaemi, T. Thio, and P. A. Wolff, "Extraordinary optical transmission through sub-wavelength hole arrays," Nature **391**(6668), 667–669 (1998).
12. "Lumerical FDTD," (Lumerical Solutions, Inc.), p. FDTD solutions.
13. R. C. Weast, *CRC handbook of chemistry and physics* (CRC Press, 1988).
14. H. Raether, *Excitation of plasmons and interband transitions by electrons* (Springer-Verlag, 1980).

#203208 - $15.00 USD Received 16 Dec 2013; revised 25 Feb 2014; accepted 26 Feb 2014; published 10 Mar 2014

15. P. B. Johnson and R. W. Christy, "Optical Constants of the Noble Metals," Phys. Rev. B **6**(12), 4370–4379 (1972).
16. L. Rayleigh, "III.Note on the remarkable case of diffraction spectra described by Prof. Wood," Philosophical Magazine Series 6 **14**(79), 60–65 (1907).
17. D. Maystre, "Theory of Wood's Anomalies," in *Plasmonics*, S. Enoch, and N. Bonod, eds. (Springer 2012), pp. 39–83.
18. N. J. Willis, *Bistatic radar* (SciTech Publishing, 2005).
19. W. A. Murray, S. Astilean, and W. L. Barnes, "Transition from localized surface plasmon resonance to extended surface plasmon-polariton as metallic nanoparticles merge to form a periodic hole array," Phys. Rev. B **69**(16), 165407 (2004).
20. G. Mie, "Contributions to the optics of turbid media, particularly of colloidal metal solutions," Contributions to the optics of turbid media, particularly of colloidal metal solutions Transl. into ENGLISH from Ann. Phys.(Leipzig), v. 25, no. 3, 1908 p 377–445 **1**, 377–445 (1976).
21. C. Sonnichsen, T. Franzl, T. Wilk, G. von Plessen, and J. Feldmann, "Plasmon resonances in large noble-metal clusters," New J. Phys. **4**, 93 (2002).
22. S. Link and M. A. El-Sayed, "Spectral properties and relaxation dynamics of surface plasmon electronic oscillations in gold and silver nanodots and nanorods," J. Phys. Chem. B **103**(40), 8410–8426 (1999).
23. P. K. Jain, K. S. Lee, I. H. El-Sayed, and M. A. El-Sayed, "Calculated absorption and scattering properties of gold nanoparticles of different size, shape, and composition: Applications in biological imaging and biomedicine," J. Phys. Chem. B **110**(14), 7238–7248 (2006).
24. W. Zhang, S. H. Brongersma, O. Richard, B. Brijs, R. Palmans, L. Froyen, and K. Maex, "Influence of the electron mean free path on the resistivity of thin metal films," Microelectron. Eng. **76**(1-4), 146–152 (2004).
25. D. Josell, S. H. Brongersma, and Z. Tokei, "Size-Dependent Resistivity in Nanoscale Interconnects," Annu. Rev. Mater. Res. **39**(1), 231–254 (2009).
26. K. Fuchs and N. F. Mott, "The conductivity of thin metallic films according to the electron theory of metals," Math. Proc. Camb. Philos. Soc. **34**(01), 100–108 (1938).
27. E. H. Sondheimer, "The mean free path of electrons in metals," Adv. Phys. **1**(1), 1–42 (1952).
28. J. van de Groep, P. Spinelli, and A. Polman, "Transparent conducting silver nanowire networks," Nano Lett. **12**(6), 3138–3144 (2012).
29. S. J. Jeong, J. E. Kim, H. S. Moon, B. H. Kim, S. M. Kim, J. B. Kim, and S. O. Kim, "Soft Graphoepitaxy of Block Copolymer Assembly with Disposable Photoresist Confinement," Nano Lett. **9**(6), 2300–2305 (2009).

1. Introduction

A transparent electrode is a critical component of many electronic devices such as liquid crystal displays, touch screens, organic light emitting diodes, solar cells, electronic books, and smart windows [1]. The most important parameters of a transparent electrode are its optical transmittance (T) and electrical sheet resistance (R_{sq}). High transmittance and low sheet resistance cannot easily be achieved simultaneously because they have a trade-off relationship. Indium tin oxide (ITO) has been widely used as the transparent electrode material in optoelectronic devices owing to its high transmittance (~90%) as well as low electrical resistance (< 100 Ω/□). However, ITO suffers from a number of serious drawbacks including high material cost due to the scarcity of indium, lack of flexibility, and damage to the organic layer during sputter deposition [2, 3]. Therefore, alternative materials such as carbon nanotube networks [4], graphene [5], and metal nanowires [6, 7] have been of interest to researchers.

Because of its high electrical conductivity at room temperature as well as low cost [8, 9], metal-based transparent electrodes are promising candidates among these alternative solutions. To simultaneously achieve high conductivity and high transmittance, much research has focused on the periodic arrangements of metal wires. In these grid structures, transmittance and conductivity can be manipulated by controlling the thickness, period, and width of metal grids [2]. Metal grids have been studied and applied as wire grid polarizers (WGPs). Polarization is strongly dependent on the WGP structure; therefore, reducing this dependency is essential for applying WGPs as transparent electrodes [10]. A metal grating with narrow slits, another example of a metal grid, exhibits extraordinary optical transmission, resulting in higher transmittance than that of the opening region, but it also exhibits low optical transmittance due to its narrow opening region (with typical sizes of only a few percent), which makes them unsuitable for use as transparent electrodes [11].

Numerical analyses of the transmittance of one-dimensional (1-D) and two-dimensional (2-D) metal grids have recently been performed to obtain the optimized design of these structures [2, 3]. These studies have only been conducted for nanoscale silver structures.

#203208 - $15.00 USD Received 16 Dec 2013; revised 25 Feb 2014; accepted 26 Feb 2014; published 10 Mar 2014

Moreover, the transmittance characteristics of different grids cannot be directly compared owing to differences in the opening ratios of the structures.

In this study, we simulated and compared the transmittance of 1-D periodic structures of Ag or Al with different widths ranging from 25 nm to 5 μm. Two configurations with opening ratios of 90% and 95%, corresponding to period-to-width ratios of 10 and 20, respectively, were considered in order to obtain high transmittance and to reduce the polarization dependency. By simulating different grid scales and materials, we clearly identified the dominant physical mechanisms that significantly affect the transmission of light through 1D metal grids.

2. Simulation background

We performed a two-dimensional (2D) electromagnetic simulation based on the finite-difference time-domain (FDTD) method [12] to analyze the physical phenomena affecting the transmission of light passing through a one-dimensional (1D) metal grid. In the FDTD method, Maxwell's equations are discretized using the central differences in time and space, and the equations are numerically solved to obtain information on optical characteristics. To identify the effect of surface plasmons on optical transmittance, silver (Ag) and aluminum (Al) were chosen as grid material as these elements have a high electrical conductivity. The simulations were conducted with the Ag and Al grid thicknesses fixed at 50 nm and without an additional substrate.

It is known that the size of the 1D metal grid structure affects its electrical properties (*e.g.*, sheet resistance R_{sq}) according to the following equation: $R_{sq} = (\rho/h)(a/w)$, where a is the period, w is the width, h is the thickness of metal grids, and ρ is the resistivity of the metal [2]. In the simulation, the sheet resistance was kept constant for a specific opening ratio (90% or 95%) because the thickness of the metal grids remained unchanged. The simulation described here was an attempt to investigate any changes in transmittance when the pattern size was changed from 25 nm to 5 μm within an area of 700 μm × 30 μm. For a 1D metal grid, the transverse electric (TE: electric field parallel to the grid) and transverse magnetic (TM: magnetic field parallel to the grid) polarizations can be analyzed independently. A power monitor was placed 10 μm from the metal network, and perfectly matched layer (PML) boundary conditions were used on the x and y axes to eliminate unexpected scattering during the simulation. The optical constants of Ag and Al were obtained from a combined Drude, Lorentz, and Debye model fitted to the data from the CRC press [13].

3. Results and discussion

3.1 Micron-scale grids

Figures 1(a) and 1(b) show the transmittance of the Ag metal grid obtained by the FDTD simulation. The peak of the transmittance located around 328 nm (~3.78 eV) in Figs. 1(a) and 1(b) can be explained by the bulk plasmon frequency of silver [14, 15]. The imaginary part of the refractive index (extinction coefficient k) for Ag is lowest at this wavelength (~0.26, inset in Fig. 1(a)), resulting in a local transmittance peak. Transmittance of the micron-scale grid can be calculated as the sum of light passing thorough the uncovered region and the light penetrating the metal grid itself. At 328 nm, the transmittance through a 50 nm-thick Ag film was calculated as 60% (inset in Fig. 1(a)). Because 60% of the light penetrates the metal-covered area (5% and 10% for opening ratios of 95% and 90%, respectively) at 328 nm and 100% of the light passes through the uncovered area (for both 95% and 90% opening ratio), the transmittance of the silver grids at 328 nm are 98% and 96% for the 95% and 90% opening ratios, respectively. Unlike Ag grids, the Al grids exhibit transmittance close to the opening ratio because a 50-nm-thick Al layer is optically opaque in the investigated wavelength range (see inset in Fig. 1(a)), as can be seen in Figs. 1(c) and 1(d), respectively). When the width of the metal grid is large, the transmittances of TE- and TM-polarized light are similar for both the Ag and Al metal grids. As shown in Fig. 1, the transmittances of TE

#203208 - $15.00 USD Received 16 Dec 2013; revised 25 Feb 2014; accepted 26 Feb 2014; published 10 Mar 2014

and TM are indeed similar for the 5-μm width metal grid, but the difference between them increases as the width becomes smaller, as shown in Fig. 2.

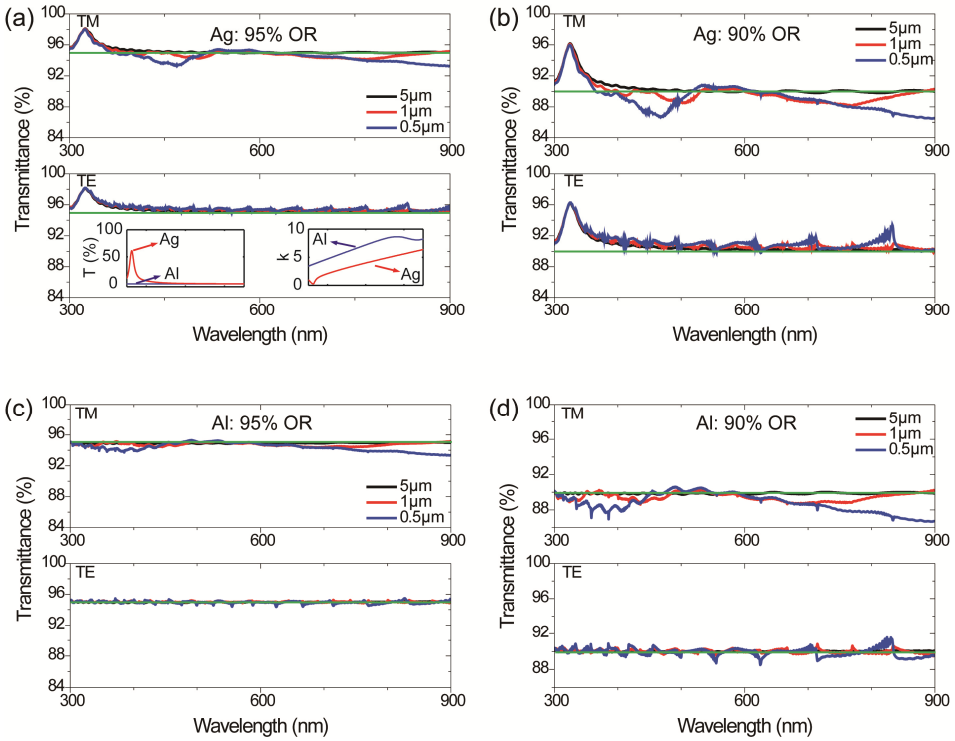

Fig. 1. Simulated optical transmittance of 1D metal grids with micron widths as a function of wavelength and polarization. (a) 95% and (b) 90% opening ratios for silver grids, (c) 95% and (d) 90% opening ratios for Al grids. The linewidths of the grids are shown in the legend. The green horizontal lines indicate the opening ratio of the structures. The inset in (a) shows the imaginary part of refractive index and the calculated transmittance of metal films of 50-nm thickness.

3.2 Nanoscale grids

Figure 2 shows the transmittances of the metal grids with pattern widths of 100 nm, 50 nm, and 25 nm and opening ratios of 95% and 90%. The most notable result is the anomalous sharp peaks of the TE mode. These peaks occur at the same wavelengths for both Ag and Al as a result of the Rayleigh anomaly [16]. A Rayleigh anomaly occurs when the order of diffraction becomes tangential to the plane of the grid. The diffracted beam intensity increases just before the diffracted order vanishes. The Rayleigh anomaly can be described by $-\sin\theta \pm 1 = n\lambda/d$, where d is the grid spacing, θ is the incident angle, and λ is the wavelength of incident light [17]. Using this equation, the maximum beam intensity is expected to occur when $\lambda = d/n$ with the incident angle being 0° (θ = 0°). For example, in Figs. 2(a) and 2(c), peaks located at 333 nm (n = 6), 400 nm (n = 5), 500 nm (n = 4), and 666 nm (n = 3) are shown; they were obtained using the Rayleigh anomaly equation at a given period of 2 μm (black line). The agreement between results in Figs. 2(a) and 2(c) and between results in Figs. 2(b) and 2(d) confirms that Rayleigh anomaly peaks occur for all metal grids at a visible wavelength.

While the anomalous peak in the nano-slit structure, which is used in the research of extraordinary optical transmission, appears in TM-polarized (TM-pol) light in accordance with Babinet's principle, its complementary structure (the grid with high opening ratio)

#203208 - $15.00 USD Received 16 Dec 2013; revised 25 Feb 2014; accepted 26 Feb 2014; published 10 Mar 2014

exhibits anomalous peaks in TE polarized (TE-pol) light [18]. The transmittances of an Al grid and nano-slit (not shown) exactly corresponds to Babinet's principle, but the result from Ag does not agree with the Babinet's principle owing to the transmittance of the Ag thin film as well as surface plasmon resonance.

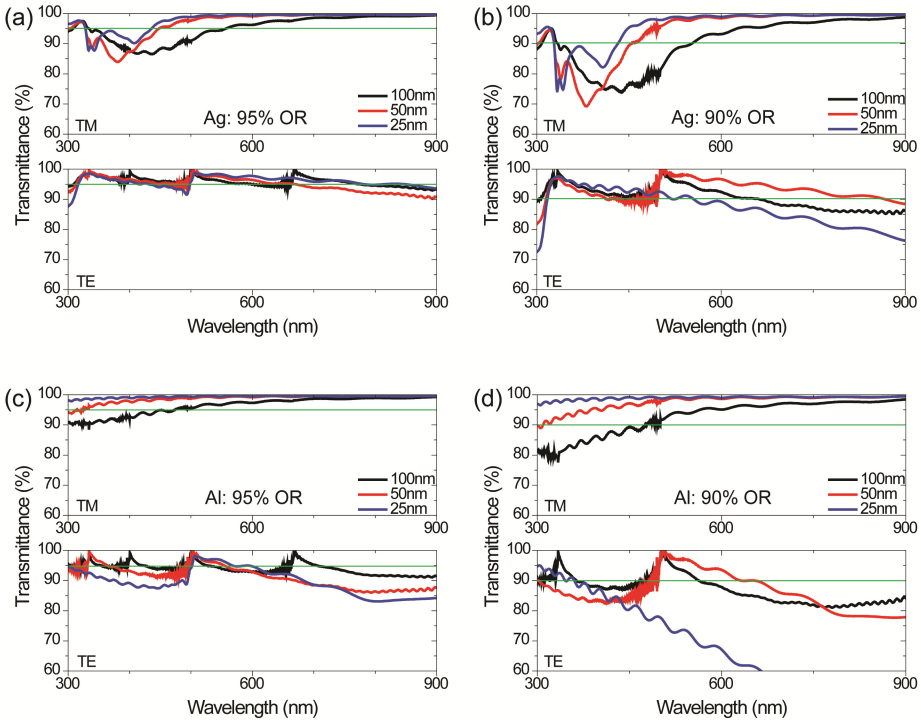

Fig. 2. Calculated optical transmittance of 1D metal grids with nanoscale widths as a function of wavelength and polarization. (a) 95% and (b) 90% opening ratio (OR) for silver grids, (c) 95% and (d) 90% OR for Al grids. The linewidths of the grids are indicated in the legend. The green horizontal line indicates the opening ratio of the structures.

Calculations for the 1D grid with a 250-nm period, i.e., a period shorter than the wavelength of visible light, were also performed. As can be seen in the blue line plot in Figs. 2(b) and 2(d), the transmittance in TE-polarized light gradually decreases for wavelengths longer than the 1st order diffraction wavelength (*e.g.*, 500 nm for 50 nm width with 90% OR), and it is directly influenced by the extinction coefficient of the metal. In Fig. 2(c), the transmittance of the 25-nm-width grid (blue line plot) is slightly increased around 800 – 900 nm, and the extinction coefficient of Al (inset in Fig. 1(a)) also slightly decreases in this wavelength range. Similarly, the transmittance in the Ag grid also gradually decreases as the extinction coefficient of Ag gradually increases. Owing to the lower k value compared to Al, the Ag grid exhibits less reduction in transmittance. This is the reason why Al with a small period is desirable for WGP application. For WGP application, the period of grid is typically set to approximately 100 nm to generate 1st order diffraction in the deep UV region, minimizing the transmittance of TE-polarization light.

In the case of TM-polarized light, the transmittance of the nanoscale grid significantly depends on the material of the grids. In contrast to the Al grid, a localized surface plasmon resonance (LSPR) can occur in the Ag grid, which causes a considerable dip in the transmission spectra [19]. Figure 3 shows the transmittance dip of the TM-polarized light in more detail and additional 2D plots of the calculated total charge density distribution in the Ag grid at the dip. There are two types of dips; one is fixed at 340 nm (red dotted circles in Fig. 3), and the other shifts its position as the width of the grid changes (blue dotted circles in Fig. 3). To determine the type of the dip, we calculated the divergence of the electric field,

#203208 - $15.00 USD Received 16 Dec 2013; revised 25 Feb 2014; accepted 26 Feb 2014; published 10 Mar 2014

which gives the total charge density at the wavelength at which the dip occurs. The distribution of the total charge density at the dip at longer wavelength (blue dotted circles) shows the effect of the dipole surface plasmon resonance and the electrical charge dipole layer in the lateral direction. The shift of this dip can be explained by Mie theory [20]. In the study of spectral position depending on the size and shape of a particle, the authors of [20] observed a red-shift with increasing cluster size for particle sizes greater than approximately 10 nm owing to electromagnetic retardation. A similar redshift has been observed in numerous previous studies [21–23].

Furthermore, the occurrence of the dip at the same position for both 95% and 90% opening ratio structures supports the previous finding that the transmittance dip at 400-500 nm is caused by LSPR; this was inferred from the fact that the wavelength at which the dip occurs depends on the width of the grid but not on the period.

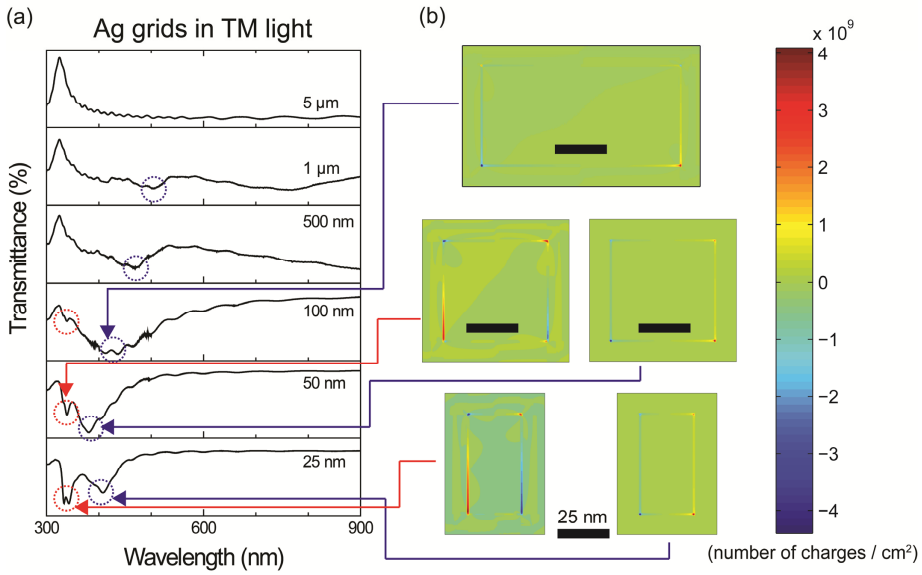

Fig. 3. Optical transmittance of the silver grid for TM-polarized light. The length in the right side of each spectrum indicates the grid width of each structure. Figure 3(b) shows the charge density of the metal grids at the transmission dip.

A dip does not occur for the Al grid with TM-polarized light owing to the absence of LSPR. Additionally, we found that higher transmittance is achieved as the wavelength increases. This trend is observed for both the 90% and 95% opening ratio structures. Figure 2(d) shows that even though all the samples had a 95% opening ratio, the average transmittances of the TM-polarized light for 100 nm, 50 nm, and 25 nm are 93.9%, 98.8%, and 99.3%, respectively. The transmittance difference in TM- and TE-polarized light allows the Al grid to be used simultaneously as a polarizer and a transparent electrode. If devices to be equipped with the grid already contain a polarizer, e.g., liquid crystal display, the Al grid would exhibit high transmittance when aligned parallel to the polarization direction of the incident light.

In terms of electrical conductivity, microscale grids are preferable to nanoscale grids. As the width of grids approaches the electron mean free path of the metal, the resistivity of metal grid increases owing to increasing surface scattering. This increase of resistivity is significant when the width of grids is narrower than 100 nm [24, 25]. Factors such as structural defects and discontinuities of the metal wire, wire-width variations, and grain boundary scattering also increase the resistivity of nanoscale grids [26, 27]. Previous research found the electrical resistivity of nanoscale grids to be 6 to 7 times higher than that of the bulk Ag and Al [28, 29].

#203208 - $15.00 USD Received 16 Dec 2013; revised 25 Feb 2014; accepted 26 Feb 2014; published 10 Mar 2014

4. Conclusions

In summary, we have investigated the transmittance of a transparent conducting electrode consisting of a periodic one-dimensional (1D) grid of silver and aluminum. Micron-width grids exhibit a transmittance value that can be predicted from the opening ratio and the transmission of the metal layer at a given wavelength. Conversely, nanoscale Ag and Al grids reveal three dominant phenomena, Rayleigh anomaly, transmission decay in TE mode, and LSPR, leading to a complex dependency of transmittance on wavelength. When the period of the grid is reduced below the wavelength of visible light, several transmission peaks caused by the Rayleigh anomaly increase the overall transmittance. Furthermore, a considerable reduction of transmittance occurs in the visible region, which is associated with extinction peaks and LSPR dips.

The physical phenomena described above make the transmittance spectra fluctuate more severely as the grid size is reduced down to the nanoscale, whereas the electrical resistance increases. Consequently we conclude that the critical feature size of conducting grids should not be less than the wavelength scale for applications as transparent electrodes in order to maintain uniform and predictable transmission characteristics as well as low electrical resistivity.

Acknowledgments

This research was supported by Basic Science Research Programs through the National Research Foundation of Korea (NRF) funded by the Ministry of Education, Science and Technology (Grant no. 2009-0083540 and 2011-0028570).

#203208 - $15.00 USD Received 16 Dec 2013; revised 25 Feb 2014; accepted 26 Feb 2014; published 10 Mar 2014